Response to RC2

July 25, 2025

We appreciate the reviewer's effort and thank them for their valuable suggestions. Reviewer 2 proposes to strengthen the manuscript by adding (1) a discussion on the Reynolds number disparity between the experiments and full-scale wind turbines and its implications, and (2) results from computational fluid dynamics (CFD) simulations to strengthen the conclusions. We agree with both suggestions and address these, as well as other minor comments, in the following.

- **Reynolds number and Mach number selection**

  As pointed out in the manuscript and by the reviewer, the inflow Mach (Ma_∞) and Reynolds (Re) numbers used in the current experimental study differ indeed from those of the IEA 15MW and 22MW reference wind turbines (RWT), see Gaertner et al. (2020) and Zahle et al. (2024), respectively. This choice is deliberate, with the purpose to reproduce qualitatively the same key physics (shock waves) as expected to occur on the full-scale wind turbine tip airfoil, while accounting for the limitations of the experimental facility as will be explained below.

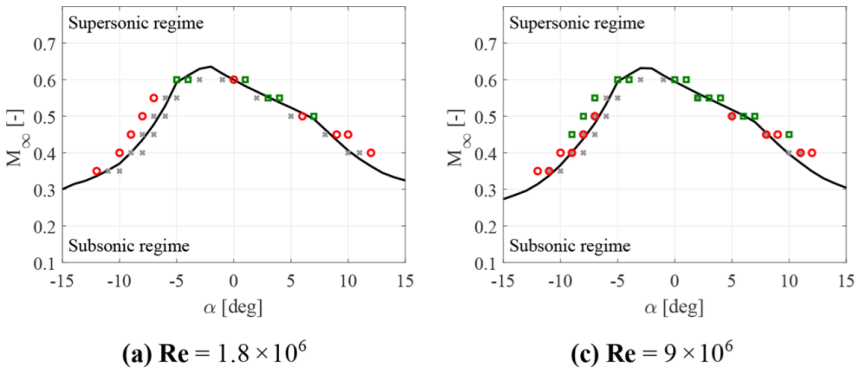

(a) Re = 1.8×10^6 **(c) Re** = 9×10^6

Figure 1: Subsonic-supersonic boundary for the FFA-W3-211 wind turbine tip airfoil, with symbols indicating URANS simulations showing no supersonic flow (grey crosses), supersonic regime established (red circles), and configurations in which shock waves appear (green squares); from Vitulano et al. (2025a).

Perhaps counter to expectation, Ma_∞ is not the single parameter relevant for the occurrence of compressibility effects, for a given angle of attack. Vitulano et al. (2025a) showed that an increase in Re plays a crucial role in accelerating the appearance of shock waves at relatively lower Ma. This is illustrated in Fig. 1. For an Re of 1.8×10^6, which is close to the Re of ca. 1.6×10^6 achieved in the current experiments, shock waves occur only at a Ma_∞ of 0.6. However, at an increased Re of 9×10^6, i.e. at full scale, shock waves start to occur already at a Ma_∞ of 0.45, close to an angle of attack of -9 deg. In addition, dynamic effects as a result of instantaneous angle of attack changes, e.g. due to turbulent gusts, can result in conditions where shock waves are observable at an even lower Ma_∞ of ca. 0.35, i.e. close to inflow Mach numbers expected at

the tip of the IEA 22MW RWT. The latter effect has been shown very recently in Vitulano et al. (2025b) using Unsteady Reynolds-Averaged Navier-Stokes (URANS) simulations of a pitching airfoil.

This combination of a very high Re, a relatively low Ma_∞ and transonic flow over the airfoil is not possible to reproduce in most, if not all, experimental wind tunnel facilities available for wind energy research. However, we currently depend on experimental studies to foster the understanding of the transonic flow dynamics of thick wind turbine airfoils, in view of the limited capability of URANS-like numerical simulation tools to capture this. Therefore, to produce shock waves on such an airfoil experimentally, we selected a combination of Ma_∞ and Re, such that the physics of shock occurrence under investigation in the experiments is qualitatively the same as expected for a full-scale turbine. We subsequently reduced Ma_∞ at the same Re to show how transonic flow without shocks can also be attained.

In the original manuscript, we briefly alluded to the argument made above when we mention the study by Vitulano et al. (2025a) on line 168. However, we agree with the reviewer that this needs to be discussed in more detail, in order to justify the selected operating conditions of the experiments. It is critical to understand that in order to reproduce the same physics of shock occurrence as in full-scale, the unavoidable reduction in Re, for any wind tunnel test, necessitates to adjust the accompanying Ma_∞ and angle of attack (see Fig. 1). Therefore, in the revised manuscript, we intend to more clearly and explicitly justify the choice of Ma_∞ and Re, including additional available but unpublished CFD analyses and experimental data that corroborate the validity of the choices made with respect to Ma_∞ and Re.

- **Supporting numerical studies**

  In the work of Vitulano et al. (2025a), URANS simulations were utilised to explore a broad parameter space for the FFA-W3-211 airfoil, viz. $0.2 \leq Ma \leq 0.7$ and $1.8 \times 10^6 \leq Re \leq 9 \times 10^6$. This allowed to identify the conditions resulting in the occurrence of shock waves, which was not possible with a low-order tool like XFOIL, and subsequently helped inform the experimental design of the current study. However, the objectives of the experiments were different, namely to investigate and characterize the unsteady nature of the resulting shock waves, which could not be captured by the URANS simulations. For this reason, the authors consider that maintaining the focus on the experimental data for the current manuscript is justified. Furthermore, the experimental data will be made available, so that it can be used to validate/design numerical models for capturing shock waves in similar conditions. A dedicated (conference) publication on validating the numerical setup used by Vitulano et al. (2025a) with our experiments is currently in preparation. Nevertheless, in line with the suggestions made by the reviewer to support conclusions and choices with simulations, we agree that including an additional section on the comparison between numerical and experimental results will form a valuable addition to the revised manuscript.

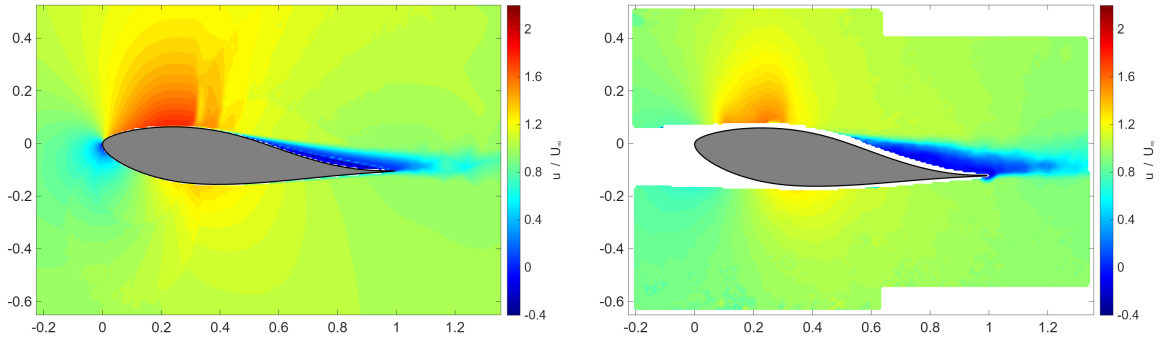

Figure 2: Normalized streamwise velocity fields for the FFA-W3-211 airfoil, for $Ma_\infty = 0.6$, AoA$= -6°$. Left: from numerical simulations (URANS, fully turbulent flow, $Re = 1.8$M); right: from experiments (tripped at 5% chord, $Re = 1.4$M).

A preview of the kind of material that will be added in the revision is shown in Fig. 2, which shows a comparison of normalized streamwise velocity fields for $Ma_\infty = 0.6$, AoA= $-10°$ obtained in simulations (left) and experiments (right). The results show a reasonable match in the overall flow physics. It is important to note that in Fig. 2, the URANS simulations were performed for a fully turbulent flow, and, to match this, the experimental data presented in this figure corresponds to a fixed-transition situation with the airfoil model tripped at 5% chord. On the other hand, the experiments presented in the current manuscript were conducted with a free-transition (untripped) airfoil model. However, the primary purpose of the data in Fig. 2 is to show that, for the same Ma_∞ and a similar Re, URANS calculations capture the mean flow field of the experiments reasonably well. This gives some confidence in using the numerical approach in order to identify the transonic flow boundary and the occurrence of shocks, also for full-scale Re. To this end, more data will be shown in the revised manuscript as detailed below.

We plan for the following additions to compare experimental results with numerical simulations:

- An analysis of the transonic envelopes (Ma_∞ vs AoA, as presented in Fig. 4 of the original manuscript) for clean (free-transition) and fixed-transition conditions using XFoil, in order to assess the impact of a transitional boundary layer on the development of local supersonic flow. This is an expansion on Fig. 1 above, calculated with URANS using existing data (or new data that can be generated rather quickly).
- A qualitative comparison between the numerical and experimental velocity flow fields will be shown, to support that both the CFD simulations and experimental measurements capture the same physical phenomena, in a time-average sense. Plots similar to Fig. 2 are intended to be provided for both $Ma_\infty = 0.6$ and 0.5, with experiments tripped and in free-transition, and CFD simulations to compare. These plots are based on already available data.

Response to additional comments and questions of the reviewer:

- Figure 4 in the original manuscript depicts the transonic envelope (the boundary between a fully subsonic flowfield and a transonic flowfield, i.e. with local regions of supersonic flow), in terms of the angle-of-attack (AoA) and the free-stream Mach number (Ma_∞) that the airfoil experiences. The latter is always subsonic ($Ma_\infty < 1$). The "supersonic" conditions refer to the occurrence of local regions of supersonic flow appearing in the flowfield around the airfoil due to flow acceleration on the suction side, which can happen even if the free-stream remains subsonic. This will be clarified in the revised manuscript.

- For $Ma_\infty = 0.5$ and AoA= $-10°$, the mean (i.e., time-average) flow is not transonic (as seen in Figure 5e). Figure 7d shows the probability of supersonic flow over the airfoil for the same conditions as Figure 5e, highlighting the fact that $\sim 30\%$ of the time, local supersonic pockets occur near the leading edge. This was already discussed in the text (line 258) and will be elaborated on in the revised manuscript for clarity.

- In Figure 8 of the original manuscript, schlieren images for $Ma_\infty = 0.55$ were added, alongside those for $Ma_\infty = 0.5$ and $Ma_\infty = 0.6$, to document Mach number effects on the flowfield, i.e. revealing the growing strength of the shocks with increasing Mach number. However, no PIV data was acquired for this intermediate case of $Ma_\infty = 0.55$, so it is not discussed elsewhere in the original manuscript. In the revised manuscript, we will further clarify the addition of this case to the schlieren analysis.

In summary, the decision to carry out the experiments in the wind tunnel at a higher Mach number, in combination with a lower Reynolds number than for full-scale, was made carefully and deliberately to balance the experimental limitations, with the goal to capture (qualitatively) the physics (of shock waves) that are expected to occur at full-scale. This will be explained in more detail in the revised manuscript. In addition, we will add available but previously unpublished data from URANS simulations to this discussion that were used to design the experiment and provide confidence in the relevance of our findings and our conclusions.

References

Gaertner, E., Rinker, J., Sethuraman, L., Zahle, F., Anderson, B., Barter, G., Abbas, N., Meng, F., Bortolotti, P., Skrzypinski, W., Scott, G., Feil, R., Bredmose, H., Dykes, K., Shields, M., Allen, C., & Viselli, A. (2020). Definition of the IEA Wind 15-Megawatt Offshore Reference Wind Turbine. *Tech. Rep., National Renewable Energy Laboratory (NREL), Golden, CO.*

Vitulano, M., De Tavernier, D., De Stefano, G., & von Terzi, D. (2025a). Numerical analysis of transonic flow over the FFA-W3-211 wind turbine tip airfoil. *Wind Energy Science*, 10(1), 103–116.

Vitulano, M., De Tavernier, D., De Stefano, G., & von Terzi, D. (2025b). CFD analysis of dynamic wind turbine airfoil characteristics in transonic flow using URANS. *Wind Energ. Sci. Discuss.*, [preprint], https://doi.org/10.5194/wes-2025-125, in review.

Zahle, F., Barlas, T., Lonbaek, K., Bortolotti, P., Zalkind, D., Wang, L., Labuschagne, C., Sethuraman, L., & Barter, G. (2024). Definition of the IEA Wind 22-Megawatt Offshore Reference Wind Turbine. *Tech. Rep., National Renewable Energy Laboratory (NREL), Golden, CO (United States).*